

# Multiple dynamical components in Local Group dwarf spheroidals

Alan W. McConnachie, Jorge Peñarrubia & Julio F. Navarro

*Department of Physics and Astronomy, University of Victoria, Victoria, B.C., V8P 1A1, Canada*

16 July 2018

## ABSTRACT

The dwarf spheroidal (dSph) satellites of the Local Group have long been thought to be simple spheroids of stars embedded within extended dark matter halos. Recently, however, evidence for the presence of spatially and kinematically distinct stellar populations has been accumulating. Here, we examine the influence of such components on dynamical models of dwarf galaxies embedded in cold dark matter halos. We begin by constructing a model of Andromeda II, a dSph satellite of M31 which shows evidence for spatially distinct stellar components. We find that the two-component model predicts an overall velocity dispersion profile that remains approximately constant at  $\sim 10 - 11 \text{ km s}^{-1}$  out to  $\sim 1 \text{ kpc}$  from the center; this is despite wide kinematic and spatial differences between the two individual components. This prediction can be validated by detailed spectroscopic analysis of this galaxy. The presence of two components may also help to explain oddities in the velocity dispersion profiles of other dSphs; we show that velocity dispersion profiles which appear to rise from the center outwards before leveling off—such as those of Leo I, Draco, and Fornax—can result from the gradual transition from a dynamically cold, concentrated component to a second, hotter, and more spatially extended one, both in equilibrium within the same dark halo. Dwarf galaxies with two stellar components generally have a leptokurtic line-of-sight velocity distribution which is well described by a double Maxwellian. This may be contrasted with other dynamical explanations such as a radially-dependent anisotropy in the stars’ orbits. Interestingly, we find that multiple equilibrium components could also provide a potential alternative origin for “extra-tidal” stars (normally ascribed to tidal effects) in situations where corroborating evidence for tides — such as elongation of the main body of the dwarf in the orbital direction or velocity gradients across its face driven by protruding tidal tails — may be lacking.

**Key words:** galaxies: dwarf — galaxies: halos — galaxies: kinematics and dynamics — Local Group — galaxies: structure

## 1 INTRODUCTION

Dwarf spheroidal (dSph) galaxies are extremely faint systems whose relatively large size and velocity dispersion combine to make them premier examples of systems likely dominated by dark matter. They contain little or no gas, and individual stars are the only available tracer of their structure and kinematics. Although long regarded as relatively simple, single-component spheroids of stars, this view has been challenged by the advent of panoramic imaging techniques and multi-object spectrographs in large telescopes.

The analysis of the color-magnitude diagrams (CMDs) of dSphs shows, in many systems, compelling evidence for multiple and protracted episodes of star formation (eg. Grebel 1997; Mateo 1998, and references therein), as well as for the presence of spatially distinct stellar populations

(Da Costa et al. 1996; Harbeck et al. 2001). These populations often spill beyond the nominal “tidal radius” estimated from King-model fits to the inner surface brightness profile (eg. Muñoz et al. 2006 and references therein), a result which has brought into focus questions regarding the role of Galactic tides in limiting the spatial extent of dSphs, as well as the mass and spatial extent of their surrounding dark matter halos (Johnston et al. 2002; Peñarrubia et al. 2007).

Spectroscopic studies have also uncovered remarkable complexity in the dynamics of dSphs. As sufficient data become available, a complex picture has arisen where kinematic oddities such as cold clumps (Kleyna et al. 2003), chemodynamically distinct stellar populations (Tolstoy et al. 2004; Battaglia et al. 2006; Ibata et al. 2006), and hints of rising dispersion profiles (Wilkinson et al. 2004; Muñoz et al. 2005; Koch et al. 2007;

arXiv:astro-ph/0608687v2 21 Jun 2007

Walker et al. 2006), are common. This is at odds with the “natural” expectation for well-mixed stellar systems, where the velocity distribution is expected to be a smooth function of radius. Observations thus suggest that it may be time to relax the standard assumption that dSphs are well described by a single well-mixed stellar system embedded within a dominant dark matter halo.

In Peñarrubia et al. (2007), we examined the observational properties of single component stellar systems (described by King models) embedded in massive cold dark matter CDM haloes (described by Navarro, Frenk & White (1996, 1997, hereafter NFW) profiles), and applied these models to the known population of Local Group dSphs. We examine here the general effect of allowing for multiple stellar components in these dynamical models. We begin in §2 by motivating the modeling technique using the case of Andromeda II (And II; a dSph companion of M31), and then examine in general the velocity dispersion and surface density profiles of two-component stellar systems embedded within a CDM halo. We conclude in §3 with a discussion of our results and their wider implications.

## 2 DYNAMICS OF MULTIPLE STELLAR COMPONENTS

### 2.1 The case of Andromeda II

And II is a dSph satellite of M31 located at a distance of  $\sim 650$  kpc from the Milky Way (McConnachie et al. 2004, 2005). McConnachie & Irwin (2006) present its surface brightness profile based on Isaac Newton Telescope wide field imaging, and suggest that a discontinuity in the profile at  $r \sim 2'$  may be evidence that it possesses a secondary “core” component.

Deeper, follow-up imaging of And II was obtained by McConnachie et al. (2007) using the Subaru Suprime-Cam wide field camera. The black squares in Figure 1 reproduce the overall radial profile of And II derived using these data. The deeper data allow the derivation of the radial profiles of distinct stellar populations; the bottom two profiles shown in the same panel trace the spatial distribution of horizontal branch stars (HB) and the reddest red-giant branch (RRGB) stars. Clearly, the HB stars are more spatially extended than the RRGB stars, which trace an exponential profile. As discussed in detail in McConnachie et al. (2007), it is very likely that these two profiles represent the density distribution of two distinct stellar components in And II. Not only does an appropriately weighted sum of these two profiles fits the overall number density profile remarkably well, as indicated in Figure 1, but it also explains significant differences seen in the stellar populations at small and large radii. The reader is referred to McConnachie et al. (2007) for more detail on these data and on the construction of these profiles.

Large differences in spatial distributions of stars should manifest themselves kinematically, and this can in principle be used to constrain the properties of the overall potential. As described by Peñarrubia et al. (2007), one expects a direct link between the velocity dispersion and the spatial distribution of stars orbiting within a CDM halo. A stellar component deeply embedded within the central regions of a CDM halo is expected to have a low central velocity dispersion and a dispersion profile that remains flat well outside

its characteristic core radius. More extended components, on the other hand, should have higher central velocity dispersions and more steeply declining dispersion profiles.

Detailed kinematic studies of And II are currently lacking. However, Côté et al. (1999) measure a central velocity dispersion of  $9.3 \pm 3$  km s $^{-1}$  based on 7 stars. Given the expected dominance of the central component in the inner few hundred parsecs of And II, it is likely that this measurement is representative of the central velocity dispersion of the exponential component found by McConnachie et al. (2007). Following the technique of Peñarrubia et al. (2007), we adopt this value and the appropriate value for the ‘core’ radius of the central component ( $r_c \sim 370$  pc) to determine the properties of a  $\Lambda$ CDM halo at  $z = 0$  compatible with these constraints. The resulting NFW profile may be fully characterized by the peak of the circular velocity curve, ( $V_{\max}, r_{\max}$ ): we find ( $V_{\max} = 17.4$  km s $^{-1}$ ,  $r_{\max} = 3.06$  kpc).

The velocity dispersion profiles of both components can then be computed, assuming isotropy, by solving Jeans’ equations separately for each component within the NFW potential. The predicted velocity dispersion profiles for And II are shown in the top right panel of Figure 1. As expected, the exponential component has a lower central velocity dispersion than the extended component and its profile declines by only  $\sim 1$  km s $^{-1}$  out to  $R \sim 1$  kpc. The more extended component, on the other hand, has a steeply declining profile, dropping from a central value of  $\sim 14.3$  km s $^{-1}$  to  $\sim 7$  km s $^{-1}$  at  $R \sim 2$  kpc. For comparison, the circular velocity profile of the NFW halo is plotted as a gray dashed line as a function of actual, not projected, radius.

The overall velocity dispersion profile of And II is given by the weighted sum of the profiles of the components. It has a central velocity dispersion of  $\sim 11$  km s $^{-1}$  which rises slightly and then declines slowly; at  $R \sim 1$  kpc, the velocity dispersion is  $\sim 10$  km s $^{-1}$ , and at  $R \sim 2$  kpc the dispersion has dropped to  $\sim 7$  km s $^{-1}$ . Varying the adopted values of ( $V_{\max}, r_{\max}$ ) by using the different constraints discussed in Peñarrubia et al. (2007) does not alter the central velocity dispersions significantly. The general shape of the overall profile of And II is similar to that expected for a one component galaxy, but here it is a result of the varying radial contribution of two dynamical components; this is very distinct from the standard interpretation of a flat dispersion profile arising from only one stellar component

Our predictions for And II are verifiable using current generations of multi-object spectrographs by obtaining spectroscopic metallicities of red giant branch stars in And II. McConnachie et al. (2007) conclude that the two components of And II have distinct metallicities, and so it should be possible to divide the red giant branch stars based on their metallicity. This technique has been successfully employed by Tolstoy et al. (2004) and Battaglia et al. (2006) to uncover kinematically distinct components in Sculptor and Fornax, respectively. Therefore, the model which we propose for And II is eminently falsifiable.

One may also resort to the *distribution* of line-of-sight velocities. If And II is largely made up of two independent equilibrium components of widely different dispersion, the velocity distribution will approach a double Maxwellian distribution whose kurtosis ( $\mu_4/\mu_2^2 - 3$ ) will be positive (leptokurtic) everywhere where both components contribute in comparable amounts to the density profile. This is shown in

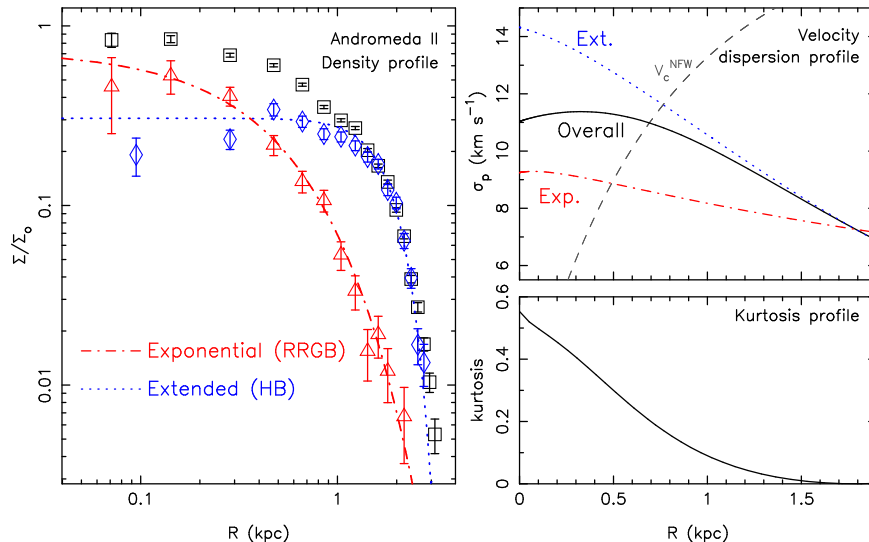


**Figure 1.** Left panel: the density profile of Andromeda II derived by McConnachie, Arimoto & Irwin (2007) (black squares). This is consistent with the sum of two spatially distinct stellar components; an extended component traced by horizontal branch stars (HB, blue diamonds/ dotted line) and an exponential component traced by the reddest red-giant branch stars (RRGB, red triangles/dot-dashed line). Upper right panel: The predicted projected velocity dispersion profile for Andromeda II (solid curve), together with the velocity dispersion profiles of the individual components, shown by dot-dashed and dotted curves. Lower right panel: the kurtosis of the line-of-sight velocity distribution as a function of radius for this model. Dwarfs with multiple equilibrium stellar components are expected to have a leptokurtic velocity distribution at all radii where both components contribute significantly.

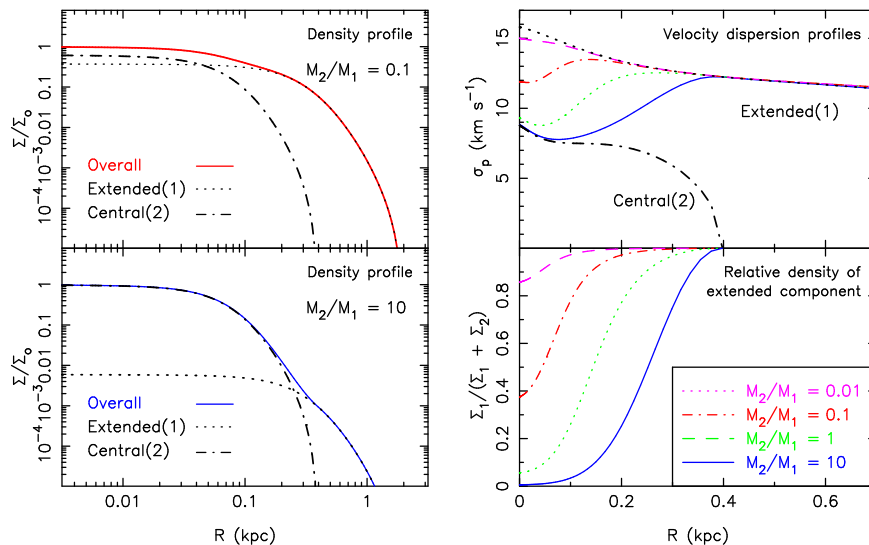


**Figure 2.** Left panel: Projected density profile of a system consisting of the superposition of two King models with mass ratios as labeled. Top right panel: Projected velocity dispersion profiles of the two stellar components and the overall projected velocity dispersion profile (line styles are as in the bottom right panel). Bottom right panel: The relative contribution of the more extended component to the total projected stellar density, shown as a function of radius for various choices of the mass ratio  $M_2/M_1$ .

the bottom right panel of Figure 1, where the kurtosis peaks at the center and declines gradually in the outer regions as the contribution from the exponential component drops. The uncertainty in the kurtosis measurement is  $\sqrt{24/N}$ , where  $N$  is the number of stars in the sample. Thus to measure the predicted value of the kurtosis in the central regions of And II to  $\sim 3 - \sigma$  will require of order 200 stars; large kinematic sample are crucial for accurate kurtosis measurements in dwarf galaxies.

## 2.2 Two-component systems

As a more general illustration of the interplay between  $\sigma_p(R)$  and multiple components, we show in the left panels of Figure 2 the density profile corresponding to two King models embedded within an NFW halo. We use King models to describe the stellar distributions here because they are a convenient means of parameterising the density profile and have been used extensively in the literature; no additional physics is implied by their usage. We set the core and tidal radii of

the more extended component to  $r_{c_1} = 400$  pc,  $r_{t_1} = 2000$  pc (dotted lines), and  $r_{c_2} = 100$  pc,  $r_{t_2} = 400$  pc (dot-dashed lines) for the more compact one. The mass ratio of the two components varies from  $M_2/M_1 = 0.1$  in the top panel to  $M_2/M_1 = 10$  in the bottom panel. The overall stellar density distribution is shown as a solid line in each panel; that of the top panel is unlikely to be observationally distinguished from a single component system in the absence of other data; the one in the bottom panel shows a “bump” in the outer density profile, not unlike those reported in some dSphs (eg. Irwin & Hatzidimitriou 1995; Sohn et al. 2006).

The top right panel of Figure 2 shows the line-of-sight velocity dispersion profile,  $\sigma_p(R)$ , corresponding to these two components (embedded in an NFW halo with  $r_{\max} = 2$  kpc and  $V_{\max} = 30$  km s $^{-1}$ ). The bottom right panel shows how the importance of the hotter, more extended component (#1) varies with  $R$  for various choices of  $M_2/M_1$ . Note that, as in the case of And II, the more extended component (#1) has a declining velocity dispersion profile, in contrast with that of the more concentrated one (#2), which remains more or less flat all the way to its tidal radius,  $r_{t_2}$ .

The detailed shape of the overall velocity dispersion profile depends on the relative contribution of the two components and on their velocity difference. The various lines in the top panel of Figure 2 illustrate this for various values of the ratio  $M_2/M_1$  (see key in the bottom right panel). When one component dominates everywhere the velocity dispersion profile is indistinguishable from a single component model. As variations in the relative contribution of the two components become more significant, however, the velocity dispersion profile starts to deviate from that for a single component system. The exact shape of the resulting  $\sigma_p(R)$  profile depends closely on  $\Sigma_1/(\Sigma_1 + \Sigma_2)$ ;  $\sigma_p(R)$  may therefore set additional constraints on the spatial properties in two component models.

### 3 DISCUSSION

In two component models, the centrally concentrated component is dynamically colder and has a decreasing influence on the overall dispersion profile as a function of radius. In the extreme case where each component dominates at different radii, we transition from a cold to a hot velocity dispersion profile. It is intriguing to note that such features in the velocity dispersion profile may not be unusual in Local Group dSphs. This is illustrated in Figure 3, where we show data for Leo I, Fornax, and Draco, compiled from the literature. In each of these three cases,  $\sigma_p$  appears to rise by about a factor of  $\sim 2$  from its central value before starting to decline again. In the case of Fornax, we refer the reader to Battaglia et al. (2006). The velocity dispersion profile of Draco has previously been fitted by Mashchenko et al. (2006) using a single stellar component with a radially varying orbital anisotropy embedded in a massive halo, and Koch et al. (2007) imply a similar anisotropy profile is required for Leo I if it resides in an NFW halo.

Klimontowski et al. (2006) suggest that that these bumps in the velocity dispersion profiles are due to tidal effects. However, we consider this unlikely for two reasons (i) as concluded by Read et al. (2006a) and Klimontowski et al.

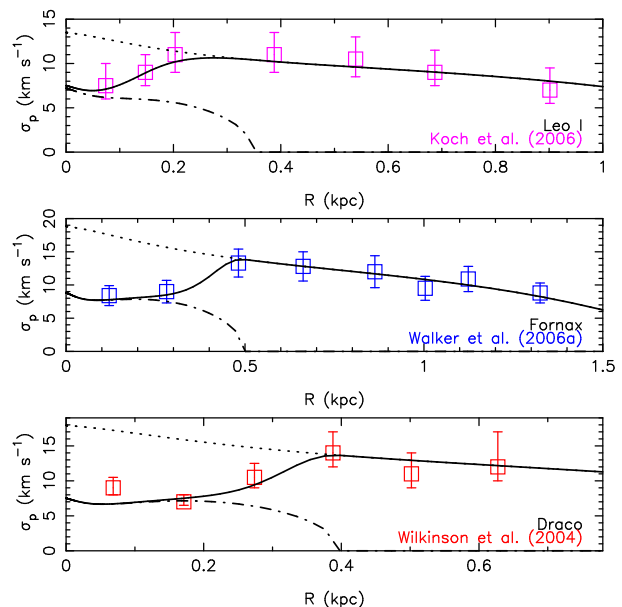


**Figure 3.** Velocity dispersion profiles of three Local Group dSphs which show a rise in their velocity dispersions from the center outwards before leveling off, taken from the literature. Possible, but degenerate, decompositions of these profiles into a cold and hot component are shown to illustrate the general plausibility of two dynamical components instead of one.

(2006), tides do not appear to affect dSph satellites inside of 1 kpc, and so are unlikely to produce observable features at radii of typically 100 – 400 pc (ii) the presence of tidally stripped stars manifest themselves as monotonically increasing features in the velocity dispersion profiles of dSphs (Read et al. 2006a; Klimontowski et al. 2006). The features highlighted in Figure 3, however, rise and then level off or decline. Thus we conclude their origin is unlikely tidal.

For each galaxy in Figure 3 we have shown a possible decomposition of the velocity dispersion profile into a cold and hot component. These curves are inevitably degenerate, given that many parameters need to be fitted to describe two stellar components and a dark matter halo. In addition, we have not attempted to determine the uncertainties due to observation errors or bin sizes since these profiles have been taken direct from the literature. Some caution is clearly required; for example, recent data for Leo I do not appear to show such a pronounced rise in the dispersion profile as found by Koch et al. (M. Mateo, private communication). As such, these curves merely demonstrate the *plausibility* of multiple components in these systems and illustrate a few fairly general conclusions that can be drawn.

The first is that the rise in  $\sigma_p$  from the center outwards reflects the rise in the relative contribution of the more extended component, a fact that may be used to constrain the relative size of the two components and to pinpoint the radius where both components contribute more or less equally to  $\sigma_p(R)$ . This is where deviations from a simple Maxwellian-like velocity distribution are likely to be maximized. At this position, the line-of sight velocity distribution would be best characterized by a double Maxwellian distribution, distinguishing it from other proposals such as

a radially-varying orbital anisotropy (see Mashchenko et al. (2006) for application of this idea to Draco).

The ratio of central-to-maximum velocity dispersion provides a lower bound to the ratio of the central velocity dispersions of the two components. Interpreting Leo I as a two-component King model, the data shown in Figure 3 suggest that the central component has a central (projected) velocity dispersion of  $\sim 6\text{--}7\text{ km s}^{-1}$ , and that the outer component has  $\sigma_{p2}(0) \sim 13\text{--}14\text{ km s}^{-1}$ . If Leo I is a multiple component system, we expect that the line-of-sight velocity distribution of stars at about  $R \simeq 150 - 200\text{ pc}$  should reveal evidence for the double Maxwellian distribution discussed previously. Similar testable inferences can be made for Fornax and Draco.

We note that a multiple component system is not required to exhibit differences in the stellar populations of its components. For example, one could build a dwarf by merging two progenitors of very different spatial extent and kinematics but similar age and metallicity. The remnant of such a merger would appear homogeneous to a CMD analysis but would retain the signature of the two progenitors in phase space. Within this context, evidence for a hierarchical origin of a dSph might be best appreciated in the dynamical evidence rather than in the CMDs.

Perhaps the most common deviation from single component models is the presence of stars that are clearly associated with the dSph, but which lie beyond the putative limiting radius of a King model fit. The presence of these “extra-tidal” stars can be caused by dynamical heating in the presence of the tidal field of the Galaxy and has attracted considerable attention because of its potential to constrain the mass and extent of a dSph’s dark halo (e.g., Johnston et al. 2002; Read et al. 2006a,b; Klimentowski et al. 2006).

As illustrated in Figure 2, the presence of a low density, extended second component, could in some instances be mistaken for “extra-tidal” stars, although in this scenario the stars are actually bound and in equilibrium with the dark matter halo. Note also that, in this interpretation, we would expect  $\sigma_p$  to *decline* in this region, since these stars belong to the extended component. Thus, a multiple component scenario offers an alternative explanation for “extra-tidal” stars in situations where corroborating evidence for tides — such as elongation of the main body of the dwarf in the orbital direction or velocity gradients across the face of the dwarf driven by protruding tidal tails — may be lacking.

If the multiple component scenario is correct, a natural question which arises from this discussion is: *how did these systems develop and preserve such complex structures?* A spatially varying star formation history, where subsequent epochs of star formation occurred in different volumes than previous ones, has been suggested by Kawata et al. (2006). Alternatively, Battaglia et al. (2006) suggest that there is tentative evidence for non-equilibrium kinematics in their data for Fornax, which might imply a merger-driven scenario. However, it is currently too soon to distinguish between these and other scenarios. Given the observational discovery of multiple structural components in dSph galaxies, it is important that the consequences for dynamical models of these systems are fully explored.

## ACKNOWLEDGMENTS

We thank Nobuo Arimoto, Mike Irwin and the DART team for assistance and useful conversations during this work. AWM is supported by a Research Fellowship from the Royal Commission for the Exhibition of 1851, and thanks Sara Ellison and Julio Navarro for additional support. We thank the referee, Mario Mateo, for useful suggestions and for sharing his data on Leo I prior to publication.

## REFERENCES

- Battaglia, G., et al. 2006, A&A, 459, 423  
 Côté, P., Mateo, M., Olszewski, E. W., & Cook, K. H. 1999, ApJ, 526, 147  
 Da Costa, G. S., Armandroff, T. E., Caldwell, N., & Seitzer, P. 1996, AJ, 112, 2576  
 Grebel, E. K. 1997, in Reviews in Modern Astronomy, ed. R. E. Schielicke, 29–60  
 Harbeck, D., Grebel, E. K., Holtzman, J., Guhathakurta, P., Brandner, W., Geisler, D., Sarajedini, A., Dolphin, A., Hurley-Keller, D., & Mateo, M. 2001, AJ, 122, 3092  
 Ibata, R., Chapman, S., Irwin, M., Lewis, G., & Martin, N. 2006, MNRAS, 373, L70  
 Irwin, M. & Hatzidimitriou, D. 1995, MNRAS, 277, 1354  
 Johnston, K. V., Choi, P. I., & Guhathakurta, P. 2002, AJ, 124, 127  
 Kawata, D., Arimoto, N., Cen, R., & Gibson, B. K. 2006, ApJ, 641, 785  
 Kleyna, J. T., Wilkinson, M. I., Gilmore, G., & Evans, N. W. 2003, ApJ, 588, L21  
 Klimentowski, J., Lokas, E. L., Kazantzidis, S., Prada, F., Mayer, L., & Mamon, G. A. 2006, astro-ph/0611296  
 Koch, A., Wilkinson, M. I., Kleyna, J. T., Gilmore, G. F., Grebel, E. K., Mackey, A. D., Evans, N. W., & Wyse, R. F. G. 2007, ApJ, 657, 241  
 Mashchenko, S., Sills, A., & Couchman, H. M. 2006, ApJ, 640, 252  
 Mateo, M. L. 1998, ARA&A, 36, 435  
 McConnachie, A., Arimoto, N., & Irwin, M. 2007, ArXiv e-prints, 705  
 McConnachie, A. W. & Irwin, M. J. 2006, MNRAS, 365, 1263  
 McConnachie, A. W., Irwin, M. J., Ferguson, A. M. N., Ibata, R. A., Lewis, G. F., & Tanvir, N. 2004, MNRAS, 350, 243  
 —. 2005, MNRAS, 356, 979  
 Muñoz, R. R., et al. 2005, ApJ, 631, L137  
 Muñoz, R. R., et al. 2006, ApJ, 649, 201  
 Peñarrubia, J., McConnachie, A., & Navarro, J. F. 2007, astro-ph/0701780  
 Read, J. I., Wilkinson, M. I., Evans, N. W., Gilmore, G., & Kleyna, J. T. 2006a, MNRAS, 367, 387  
 —. 2006b, MNRAS, 366, 429  
 Sohn, S. T., et al. 2006, astro-ph/0608151  
 Tolstoy, E., et al. 2004, ApJ, 617, L119  
 Walker, M. G., Mateo, M., Olszewski, E. W., Bernstein, R., Wang, X., & Woodroffe, M. 2006, AJ, 131, 2114  
 Wilkinson, M. I., Kleyna, J. T., Evans, N. W., Gilmore, G. F., Irwin, M. J., & Grebel, E. K. 2004, ApJ, 611, L21